Appl Phys A (2014) 114:509–513
DOI 10.1007/s00339-013-7718-z

Applied Physics A
Materials Science & Processing

Effects of oxygen plasma treatment on the surface properties of Ga-doped ZnO thin films

Ya Xue · Haiping He · Yizheng Jin · Bin Lu · Hongtao Cao · Jie Jiang · Sai Bai · Zhizhen Ye

Received: 20 October 2012 / Accepted: 18 April 2013 / Published online: 27 April 2013

Abstract We report that oxygen plasma treatment significantly changes the surface properties of Ga-doped ZnO (GZO) thin films, leading to an increase of work function and a large reduction in contact angles. We attribute the increase of work function of the GZO thin films after oxygen plasma treatment to both the lowering of the Fermi level and the shift in ionization potential.

1 Introduction

Transparent conducting oxides (TCOs) are widely used as transparent electrodes in optoelectronic devices, such as solar cells, light-emitting diodes, laser diodes, and thin-film transistors, owing to the unique combination of high electrical conductivity and excellent visible transparency [1–5]. Zinc oxide (ZnO)-based TCOs possess the advantages of low cost, earth abundance, and non-toxicity compared with the most popular of the indium oxide based TCOs, i.e. tin-doped indium oxide (ITO) [6]. ZnO is commonly doped with group-III elements, such as Al or Ga, to enhance its electrical conductivity [7, 8]. Our group and many other research groups demonstrated that Ga is a decent dopant for producing high-quality n-type ZnO because Ga atoms cause little distortion of the ZnO lattice when they are in substitutional sites [9–13].

Surface properties are key factors for TCOs, apart from electrical conductivity and visible transparency, when integrating TCOs into organic based optoelectronic devices such as organic light-emitting diodes and organic solar cells. The band alignment at the interfaces of organic semiconductors and TCOs is expected to depend directly on the work functions of the TCOs [14, 15]. The surface wetting properties of the TCOs may impact their compatibility with the organic semiconductors. In the research community of organic optoelectronics, a number of strategies, such as use of self-assembled monolayers and UV ozone treatment, were developed to modify the surface properties of the ITO electrodes and improve the device performances [16–19]. Nevertheless, few investigations have been reported on the surface modifications of the properties of Ga-doped ZnO (GZO) thin films, which are critical for future practical applications.

In this study we utilized oxygen plasma treatment to modify the surfaces of GZO thin films. Oxygen plasma treatment is one of the most widely used post-treatment methods in terms of modifying the surface properties of oxide thin films, such as ITO, TiO_2, and ZnO thin films [20–22]. The effects of oxygen plasma treatment on the surface properties, i.e. work functions and wetting properties, of the GZO thin films were investigated by means of ultraviolet photoemission spectroscopy (UPS) and contact angle measurements. The optical, electrical, and chemical bonding states of the GZO thin films were also characterized.

Y. Xue · H. He · Y. Jin (✉) · B. Lu · J. Jiang · S. Bai · Z. Ye
State Key Laboratory of Silicon Materials,
Department of Materials Science and Engineering,
Zhejiang University, Hangzhou 310027,
People's Republic of China
e-mail: yizhengjin@zju.edu.cn
Fax: +86-571-87952625

Z. Ye (✉)
e-mail: yezz@zju.edu.cn

Y. Xue · H. He · Y. Jin · B. Lu · J. Jiang · S. Bai · Z. Ye
Cyrus Tang Center for Sensor Materials and Applications,
Zhejiang University, Hangzhou 310027,
People's Republic of China

H. Cao
Ningbo Institute of Material Technology & Engineering
(NIMTE), Chinese Academy of Sciences (CAS), Ningbo 315201,
People's Republic of China

2 Experimental

The ZnO and GZO thin films were deposited by pulsed laser deposition (PLD) on quartz substrates which were pre-cleaned by ultrasonication in acetone and then ethanol. A KrF excimer laser (Compex 102, 248 nm, 25 ns) was used as the ablation source. A target for the deposition of oxide thin films was fabricated by sintering a mixture of high-purity ZnO (16.28 g, 4 N) and Ga_2O_3 (0.987 g, 4 N) powders. The laser beam was focused on the target with an energy density of about 3 J/cm^2 and a repetition rate of 5 Hz. The substrate with an area of 20.3 cm^2 was located at 4.5 cm away from the target. Both the target and the substrate were rotated during irradiation. The Ga content in the target was set to be 5 at.%. The chamber was evacuated to a base pressure of 5×10^{-3} Pa before deposition. Then high-purity O_2 (5 N) was introduced to the chamber and the pressure was kept at 5 Pa. The substrates were kept at 500 °C during the growth of the thin films. The deposition time was set to be 30 min for all samples. The as-grown films were treated by oxygen plasma for 5 min at a power of 600 W.

UPS (He I excitation source) and X-Ray photoelectron spectroscopy (XPS, with a monochromatic Al Kα source, 15 kV/8 mA) characterizations were performed using a Kratos Axis-Ultra spectrometer [23], with the Fermi energy (E_F) calibrated using an atomically clean silver sample. The contact angles of the oxide thin films were measured by a surface tension–contact angle meter (GBX DIGIDROP). The optical transmission spectra were recorded by a Shimadzu UV-3600 spectroscope. The crystal structure of the films was analyzed by X-ray diffraction (XRD) using a Bede D1 system with Cu K_α radiation ($\lambda = 0.1541$ nm). Hall-effect measurements were carried out in the van der Pauw configuration (Bio-RAD HL5500PC) at room temperature under the magnetic field of 0.32 T.

3 Results and discussion

Figures 1a and 1b show the cross-section and surface features for a typical GZO thin film. The columnar structure of the GZO thin film with highly compact grains, approx. 50–80 nm in size, can be observed. The thickness of the GZO film was determined to be ~350 nm. Figure 1c displays the XRD patterns of the as-deposited GZO and pure ZnO thin films with intensity expressed in logarithmic coordinates. The two strong peaks in the XRD pattern of the GZO thin film correspond to the (002) and (004) planes of wurtzite ZnO, respectively, implying a high preferential *c*-axis orientation. The (002) peak of the GZO thin film (at 34.5°) slightly shifts (0.2°) to a higher angle compared with that of pure ZnO (at 34.3°), in line with the substitution of Zn^{2+} (0.074 nm) by Ga^{3+} (0.062 nm), which has a smaller ionic radius. The content of Ga in the as-deposited films was determined to be 8.5 ± 1.5 at.% by XPS analysis. A possible explanation is that Zn is more volatile at the growth temperature (the saturated vapor pressure of Zn is higher than that of Ga) and therefore the content of Ga in the GZO thin films is higher than that of the target [24].

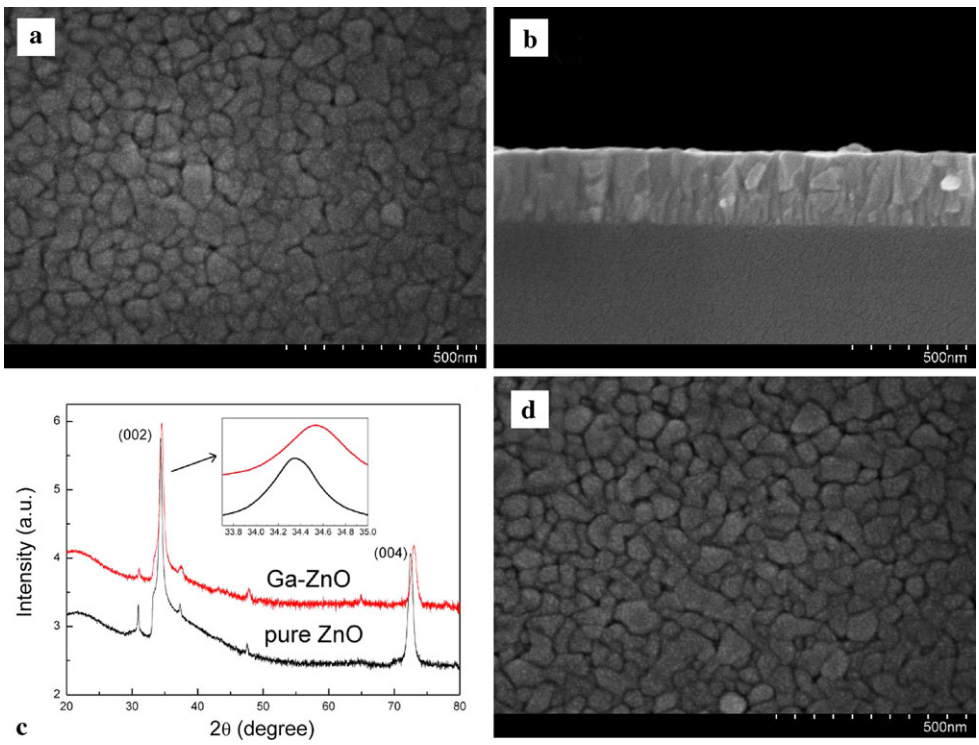

Fig. 1 (**a**) Top view of the GZO thin film before plasma treatments. (**b**) Cross-section view and (**c**) XRD pattern of the as-deposited pure ZnO and GZO thin films. The *inset* displays details of the ZnO (002) peaks. (**d**) Top view of the GZO thin film after plasma treatments

The effects of oxygen plasma treatment on the surface properties of GZO thin films are shown in Fig. 2. In the UPS spectra, the secondary electron onset, referenced to the 21.2 eV helium source, provided a direct measurement of the sample's work function, revealing that the work function of the GZO thin film was increased from 4.0 ± 0.1 to 4.3 ± 0.1 eV after the oxygen plasma treatment. The valence-band offset at the low binding energy corresponded to the energy difference between the Fermi level and the conduction-band maximum, which can be used to determine the ionization potential of the thin films. The ionization potentials for the GZO thin film before and after oxygen plasma treatment were 7.5 ± 0.1 and 7.7 ± 0.1 eV, respectively, suggesting modification of surface dipoles.

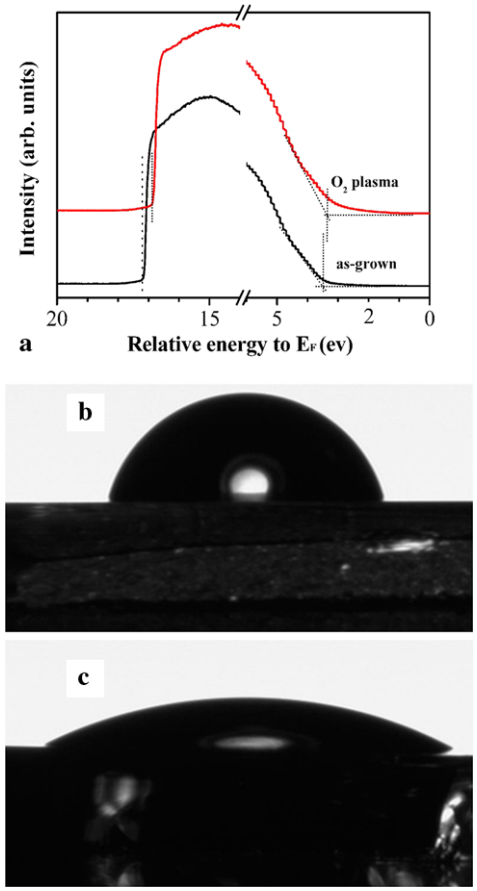

Fig. 2 (**a**) UPS spectra of the GZO thin films. (**b** and **c**) Contact angle measurements of water on the GZO thin films

The static contact angles of water on the GZO thin films are illustrated in Figs. 2b and 2c, indicating a significant reduction, from 76 to 28°, due to the oxygen plasma treatment. We also conducted static contact angle measurements with ethylene glycol and calculated the surface energies of the thin films by using the Young–Dupré equation [25]. The results (shown in Table 1) indicate that the surface energy of the GZO thin films increased from 29 to 74 mN/m after the oxygen plasma treatment. The increased surface energy of the GZO thin films may be beneficial for a number of future applications. For example, Friend and coworkers suggested that for ITO electrodes, a higher surface energy provides a better adhesion of the polymer and reduces the interfacial tension between the polymer and the substrate, which is desirable for the fabrication of polymer light-emitting diodes [26]. We note that oxygen plasma treatment did not cause significant changes in terms of surface morphology, as evidenced by the scanning electron microscope observation shown in Fig. 1d.

We investigated the effects of oxygen plasma treatment on the optical and electrical properties of the GZO thin films. As depicted in Fig. 3, the GZO thin film subjected to oxygen plasma treatment exhibits an average transmittance of about 90 % in the visible region and a sharp absorption edge in the UV region of 300–400 nm. This suggests that the superior visible transmittance properties of the GZO thin films are preserved after oxygen plasma treatment. The relationship between $(\alpha h\nu)^2$ and $h\nu$ is plotted in the inset of Fig. 3 in order to determine the optical band gap, i.e. $E_{g(opt)}$, of the samples. The $E_{g(opt)}$ values can be obtained by extrapolating the linear portion to the photon energy axis in that figure, which are 3.47 and 3.45 eV for as-grown and oxygen plasma treated GZO thin films, respectively, suggesting a shift of 20 meV to the lower energy region. The electrical properties of the GZO thin films were characterized by Hall-effect measurements. The results are summarized in Table 2. The resistivity, carrier concentration, and carrier mobility of the GZO thin films changed from 4.3×10^{-3} to 2.1×10^{-2} Ω cm, 1.2×10^{20} to 2.1×10^{19} cm^{-3}, and 12 to 14.7 cm^2/V s, respectively. We suggest that the band-gap shift was due to the combined effects of band-gap widening caused by Burstein–Moss effects and band-gap narrowing induced by band-gap renormalization [27].

As suggested by one of the reviewers, we also carried out experiments of annealing the GZO films in an oxy-

Table 1 Surface tension components of standard liquids and static contact angle of the standard liquids on the GZO films before and after the oxygen plasma treatment

Liquid	Surface tension (mN/m)			Static contact angle (°)	
	γ_L	γ_L^d	γ_L^p	Before the treatment	After the treatment
Water	72.8	21.8	51.0	76	28
Ethylene glycol	48.3	29.3	19	68	22

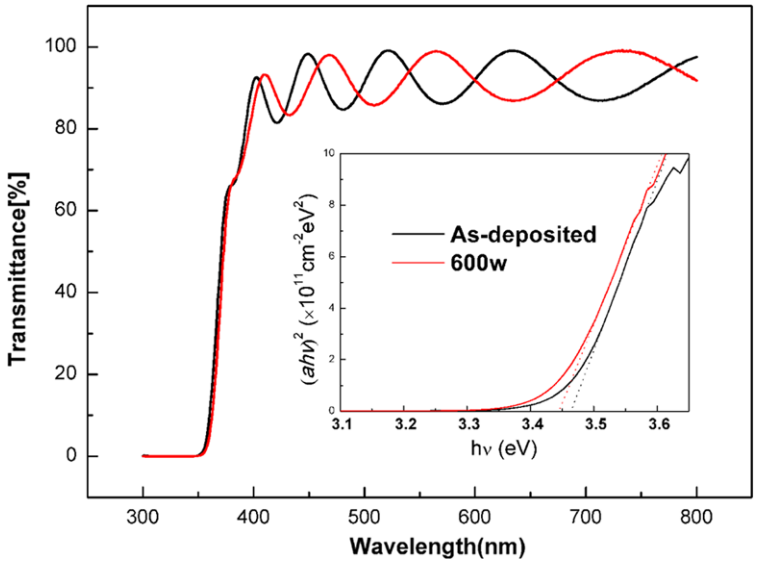

Fig. 3 Transmission spectra of the GZO thin films. The *inset* shows the plot of $(\alpha h\nu)^2$ of the GZO thin films as a function of the photon energy

Table 2 Hall-effect results: electrical properties of the GZO thin films

Sample	Electron concentration (cm^{-3})	Resistivity (Ω cm)	Mobility (cm^2/V s)	Carrier type
As-deposited film	1.2×10^{20}	4.3×10^{-3}	12	n
After annealing	1.3×10^{20}	3.7×10^{-3}	13	n
After treatment for 600 W/5 min	2.1×10^{19}	2.1×10^{-2}	14.7	n

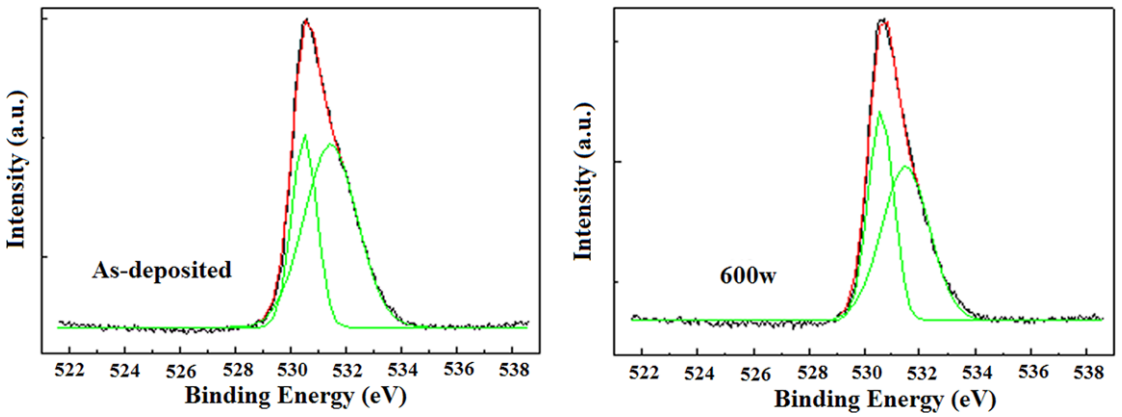

Fig. 4 The curve-fitted results of O 1*s* XPS spectra of the GZO thin films

gen atmosphere (5 Pa) at 150 °C for 5 min in order to determine the effects of oxygen annealing on the surface properties of the GZO thin films. The static contact angle (water) and the work function of the GZO films after oxygen annealing were 78° and 4.0± 0.1 eV, respectively. Hall-effect measurements showed that the resistivity and carrier concentration for the GZO films after annealing were 3.7×10^{-3} Ω cm and 1.3×10^{20} cm^{-3}, respectively (Table 2). These results indicate that the oxygen annealing procedure did not significantly change the electrical and surface wetting properties of the GZO thin films. We note that for ZnO-based TCO thin films, oxygen annealing may be effective at high annealing temperatures, i.e. ≥400 °C. For example, Deng et al. reported that the resistivity of aluminum-doped zinc oxide (AZO) thin films was increased from 1×10^{-4} to 2×10^{-4} Ω cm after annealing in oxygen for 1 h at 500 °C [28].

We carried out XPS analyses to examine the changes of chemical bonding states due to the oxygen plasma treatment. Figure 4 displays narrow-scan XPS spectra of the O 1*s* core level for the GZO thin films, which exhibit asymmetric line shapes. The peak with lower binding energy

(530.5 ± 0.1 eV) corresponds to oxygen atoms in a ZnO matrix, i.e. O–Zn bonding. The second peak, at 531.5 ± 0.1 eV, is attributed to oxygen-deficient components, such as oxygen vacancies, O–H, C–O, or loosely bound oxygen on the surface of the GZO thin films. The relative magnitude of the low-binding-energy O atoms was 0.48 in the as-deposited sample and increased to 0.71 after oxygen plasma treatment, indicating that oxygen plasma treatment was effective in terms of suppressing surface contamination and improving surface stoichiometry.

We attribute the increase of work function after oxygen plasma treatment to both the lowering of the Fermi level and the shift in ionization potential. The lowering of the Fermi level is due to the decrease of free-carrier concentration, as shown by the Hall-effect measurements. A simple estimation by assuming that the effective mass of ZnO is $0.32m_e$ and using parabolic conduction band edges suggests that the Burstein–Moss shifts for the GZO thin films before and after oxygen plasma treatment are 0.28 and 0.09 eV, respectively [29, 30]. As shown by the UPS spectra, the ionization potential for the GZO thin films is approx. 0.2 eV deeper after oxygen plasma treatment. This is in line with the increase of the components of O–Zn bonding in the XPS spectra, which suggests that oxygen plasma treatment effectively removes the surface contaminants and improves the surface stoichiometry [31].

4 Conclusions

In summary, oxygen plasma treatment significantly changes the surface properties of Ga-doped ZnO thin films, leading to an increase of work function and a large reduction in contact angles. We found no degradation of the superior transmittance properties of the GZO thin films subjected to the oxygen plasma treatment. We attribute the increase of work function of the GZO thin films after oxygen plasma treatment to both the lowering of the Fermi level and the shift in ionization potential.

Acknowledgements This work is financially supported by the National Natural Science Foundation of China (51172203, 51172204, and 51002134), the National High Technology Research and Development Program of China (2011AA050520), and the Natural Science Funds for Distinguished Young Scholars of Zhejiang Province (R4110189).

References

1. S. Suzuki, T. Miyata, M. Ishii, T. Minami, Thin Solid Films **434**, 14 (2003)
2. M. Kon, P.K. Song, Y. Shigesato, P. Frach, S. Ohno, K. Suzuki, Jpn. J. Appl. Phys. **42**, 263 (2003)
3. S. Nakamura, M. Senoh, S. Nakahama, N. Iwasa, T. Yamada, T. Matsushita, Y. Sugimoto, H. Kiyoku, Appl. Phys. Lett. **69**, 1477 (1996)
4. H. Ohta, K. Kawamura, M. Orita, M. Hirano, N. Sarukura, H. Hosono, Appl. Phys. Lett. **77**, 475 (2000)
5. P.F. Carcia, R.S. McLean, M.H. Reilly, G. Nunes, Appl. Phys. Lett. **82**, 1117 (2003)
6. K. Ellmer, J. Phys. D, Appl. Phys. **34**, 3097 (2001)
7. T. Minami, H. Sato, S. Takata, Jpn. J. Appl. Phys. **24**, 781 (1985)
8. T. Minami, Mater. Res. Soc. Bull. **25**(8), 38 (2000)
9. S.J. Henley, M.N.R. Ashfold, D. Cherns, Surf. Coat. Technol. **177**, 271 (2004)
10. Q.B. Ma, Z.Z. Ye, H.P. He, S.H. Hu, J.R. Wang, L.P. Zhu, Y.Z. Zhang, B.H. Zhao, J. Cryst. Growth **304**, 64 (2007)
11. S.M. Park, T. Ikegami, K. Ebihara, Thin Solid Films **513**, 90 (2006)
12. G.D. Yuan, W.J. Zhang, J.S. Jie, X. Fan, J.X. Tang, I. Shafiq, Z.Z. Ye, C.S. Lee, S.T. Lee, Adv. Mater. **20**, 168 (2008)
13. J.L. Zhao, X.W. Sun, H. Ryu, Y.B. Moon, Opt. Mater. **33**, 768 (2011)
14. H. Ishii, K. Sugiyama, E. Ito, K. Seki, Adv. Mater. **11**, 605 (1999)
15. W.R. Salaneck, M. Lögdlund, M. Fahlman, G. Greczynski, T. Kugler, Mater. Sci. Eng., R Rep. **34**, 121 (2001)
16. C. Yan, M. Zharnikov, A. Gölzhäuser, M. Grunze, Langmuir **16**, 6208 (2000)
17. S.Y. Kim, J.L. Lee, K.B. Kim, J. Appl. Phys. **95**, 2560 (2004)
18. J.S. Kim, F. Cacialli, R. Friend, Thin Solid Films **445**, 358 (2003)
19. M.S. Kang, H. Ma, H.L. Yip, A.K.Y. Jen, J. Mater. Chem. **17**, 3489 (2007)
20. S. Bai, Z.W. Wu, X.L. Xu, Y.Z. Jin, B.Q. Sun, X.J. Guo, S.S. He, X. Wang, Z.Z. Ye, H.X. Wei, X.Y. Han, W.L. Ma, Appl. Phys. Lett. **100**, 203906 (2012)
21. S. Gan, Y. Liang, D.R. Baer, Surf. Sci. Lett. **459**, 498 (2000)
22. M.J. Liu, H.K. Kim, Appl. Phys. Lett. **84**, 173 (2004)
23. W.Y. Wang, Q.Y. Feng, K.M. Jiang, J.H. Huang, X.P. Zhang, W.J. Song, R.Q. Tan, Appl. Surf. Sci. **257**, 3884 (2011)
24. S.S. Lin, H.P. He, Y.F. Lu, Z.Z. Ye, J. Appl. Phys. **106**, 093508 (2009)
25. M.C. Michalski, J. Hardy, B.J.V. Saramago, J. Colloid Interface Sci. **208**, 319 (1998)
26. J.S. Kim, R.H. Friend, F. Caciallia, J. Appl. Phys. **86**, 2774 (1999)
27. J.G. Lu, S. Fujita, T. Kawaharamura, H. Nishinaka, Y. Kamada, T. Ohshima, Z.Z. Ye, Y.J. Zeng, Y.Z. Zhang, L.P. Zhu, H.P. He, B.H. Zhao, J. Appl. Phys. **101**, 083705 (2007)
28. X.R. Deng, H. Deng, M. Wei, J.J. Chen, J. Mater. Sci., Mater. Electron. **23**, 413 (2012)
29. K. Ellmer, A. Klein, B. Rech, *Transparent Conductive Zinc Oxide: Basics and Applications in Thin Film Solar Cells* (Springer, Berlin, 2008)
30. J. Hu, R.G. Gordon, Mater. Res. Soc. Symp. Proc. **242**, 743 (1992)
31. Z.Z. You, J. Electron Spectrosc. Relat. Phenom. **160**, 29 (2007)